Neuron, Volume *66*

Supplemental Information

Metaplasticity at Single Glutamatergic Synapses

Ming-Chia Lee, Ryohei Yasuda, and Michael D. Ehlers

INVENTORY OF SUPPLEMENTAL INFORMATION

Figure S1 is related to Figure 1.

Figure S2 is related to Figure 2.

Figure S3 is related to Figure 3.

Figure S4 is related to Figure 6.

SUPPLEMENTAL FIGURES AND LEGENDS

Figure S1, related to Figure 1.

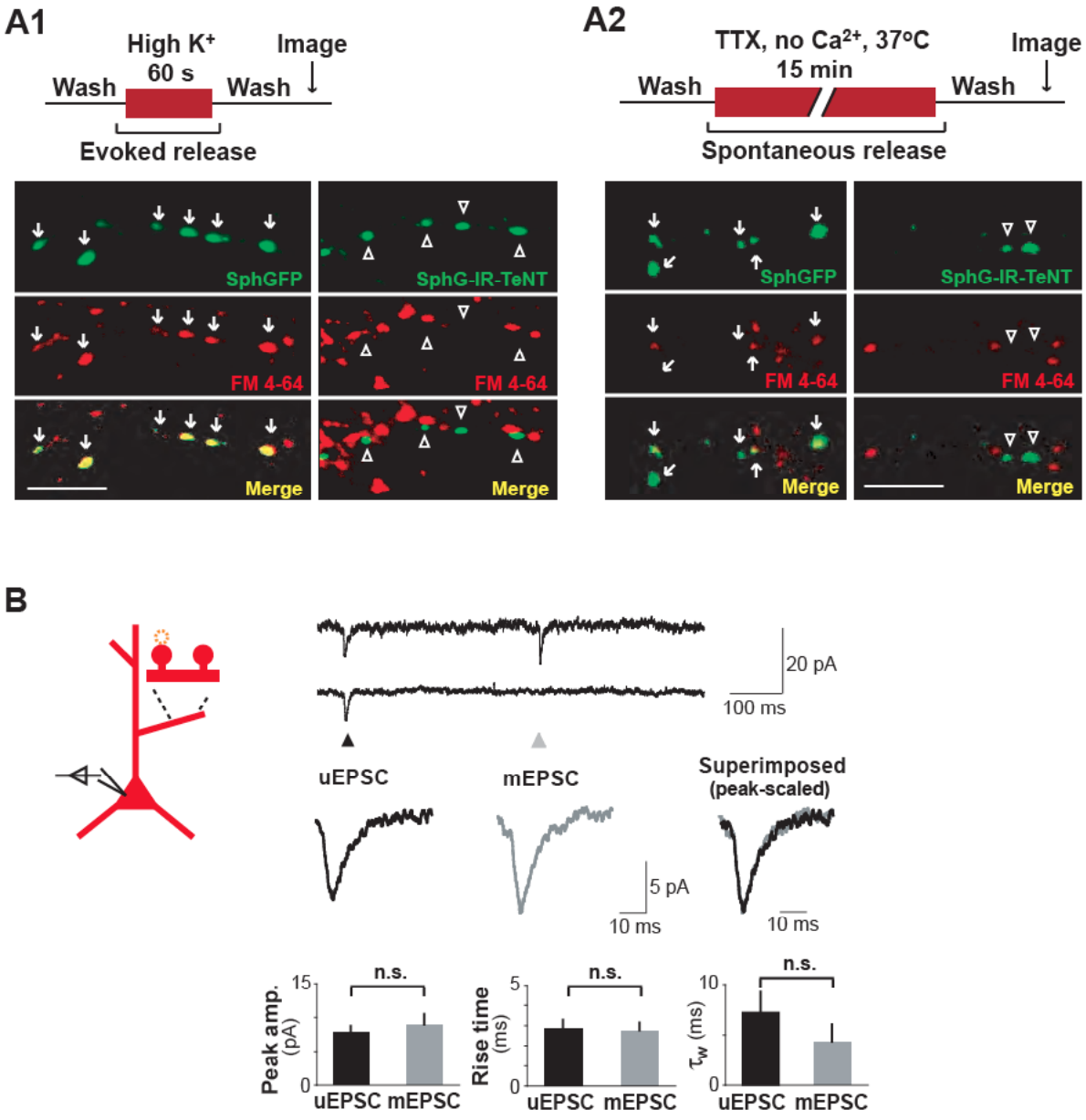

(A) Individual TeNT-silenced boutons display decreased presynaptic release and synaptic vesicle recycling. (A1) evoked release at individual boutons was monitored by depolarization-induced uptake of FM dye using high K^+ solution. Loaded FM 4-64 was visualized in presynaptic boutons expressing either synaptophysin-GFP (SphGFP,

arrows, left) or SphGFP-IRES-TeNT (SphG-IR-TeNT, arrowheads, right). Nearly all control boutons expressing SphGFP were capable of evoked release (FM-positive, 85 ± 5%). In contrast, boutons expressing SphGFP-IRES-TeNT exhibited a nearly 9-fold reduction in FM labeling upon high K^+ depolarization (FM-positive, 9 ± 3%). (A2) spontaneous release at individual boutons was monitored by FM-dye uptake in the presence of TTX. FM4-64 uptake was assayed after 15 min of spontaneous release in Ca^{2+}-free solution with TTX blockade. Whereas 31 ± 4 % of SphGFP boutons exhibited detectable spontaneous release within the 15 min time window (left, arrows), only 11 ± 5 % of boutons expressing SphGFP-IRES-TeNT were FM positive, indicating impaired spontaneous release in TeNT boutons. Scale bar, 5 μm.

(B) Focal two-photon glutamate uncaging mimics miniature events. Two-photon glutamate uncaging was performed at individual dendritic spines (dashed orange circle) while recording both uncaging-evoked excitatory postsynaptic currents (uEPSCs) and miniature excitatory postsynaptic currents (mEPSCs) under voltage clamp. Example traces indicating uEPSCs (black arrowhead) and mEPSCs (grey arrowhead) in individual recordings at -70 mV. Averaged uEPSCs (black) and mEPSCs (gray) shown individually and as superimposed traces scaled to the peak current amplitude. Data represent means ± SEM of peak amplitude (uEPSC, 7.8 ± 0.8 pA; mEPSC, 8.9 ± 1.5 pA; $p = 0.56$), rise time (uEPSC, 2.9 ± 0.4 ms; mEPSC, 2.8 ± 0.4 ms; $p = 0.85$) and decay kinetics (τ_W, uEPSC, 4.3 ± 1.7 ms; mEPSC, 7.1 ± 2.1 ms; $p = 0.32$). No significant difference was detected between uEPSCs ($n = 5$) and mEPSCs ($n = 7$), indicating that pulses of glutamate uncaging were comparable to quantal release events. n.s., not significant.

Figure S2, related to Figure 2.

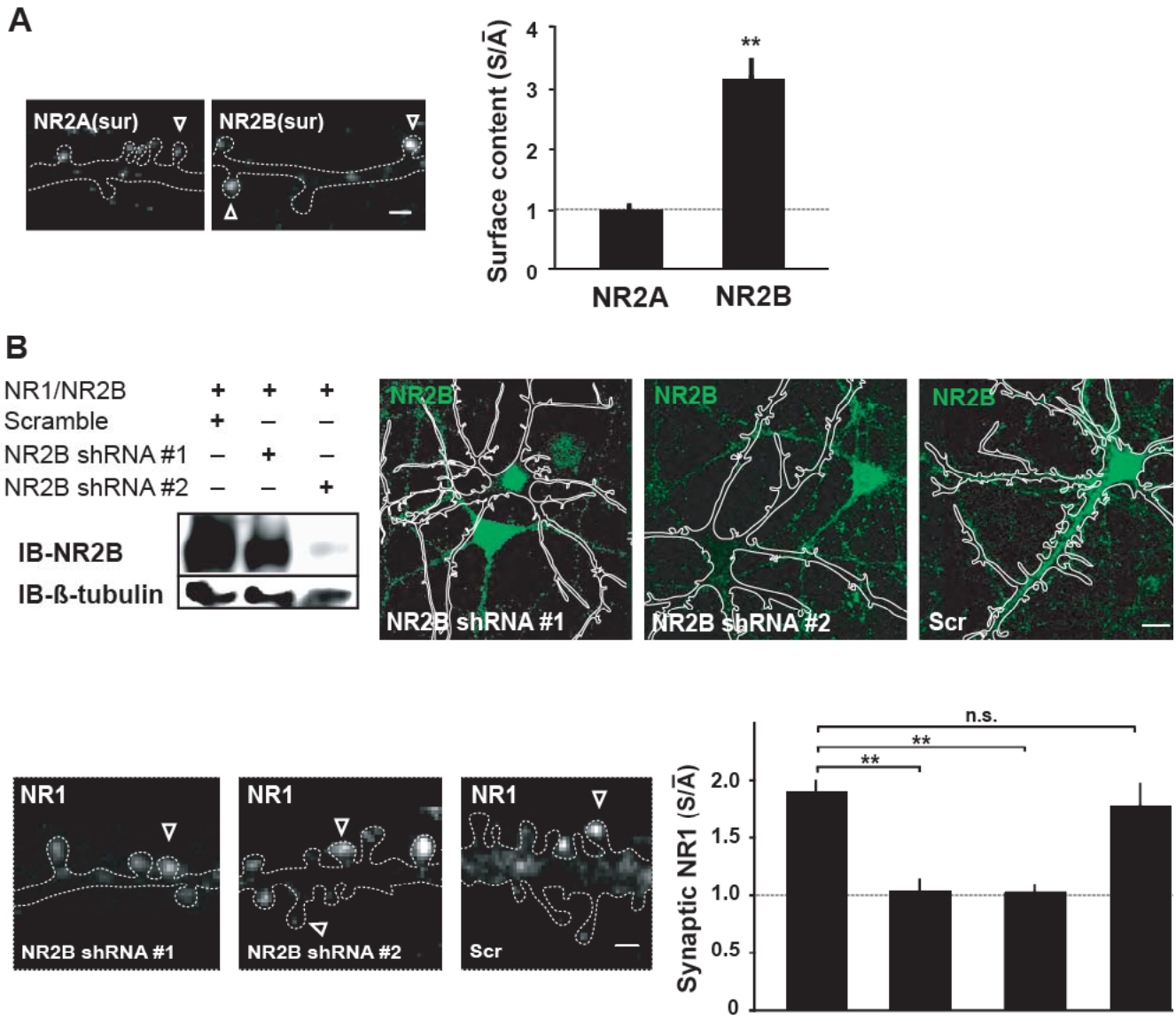

(A) Silenced synapses (arrowheads) accumulate more surface NR2B but not NR2A compared to neighboring active synapses ($S/\overline{A}$: NR2A, 1.07 ± 0.04, n = 15; NR2B, 3.07 ± 0.29, n = 34; **p < 0.01.) Scale bar, 1 μm.

(B) NR2B is required for blockade-induced accumulation of NMDARs at single synapses. As shown by immunoblot (IB) analysis, two independent NR2B shRNA sequences but not the scrambled shRNA control reduce NR2B expression in 293T cells.

β-tubulin was used a loading control here. Moreover, endogenous NR2B is effectively knocked down in hippocampal neurons by NR2B shRNA expression (transfected neurons are traced by white lines). Scale bar, 10 μm. Interestingly, NR2B knock down prevents the differential NR1 accumulation between silenced (arrowheads) and active synapses ($S/\overline{A}$: Ctrl, 1.9 ± 0.1, n = 39 neurons; NR2B shRNA#1, 1.0 ± 0.1, n = 12; NR2B shRNA#2, 1.0 ± 0.1, n = 14; Scrambled (Scr), 1.7 ± 0.2; **p <0.01; n.s., not significant). Scale bar, 1 μm.

Figure S3, related to Figure 3.

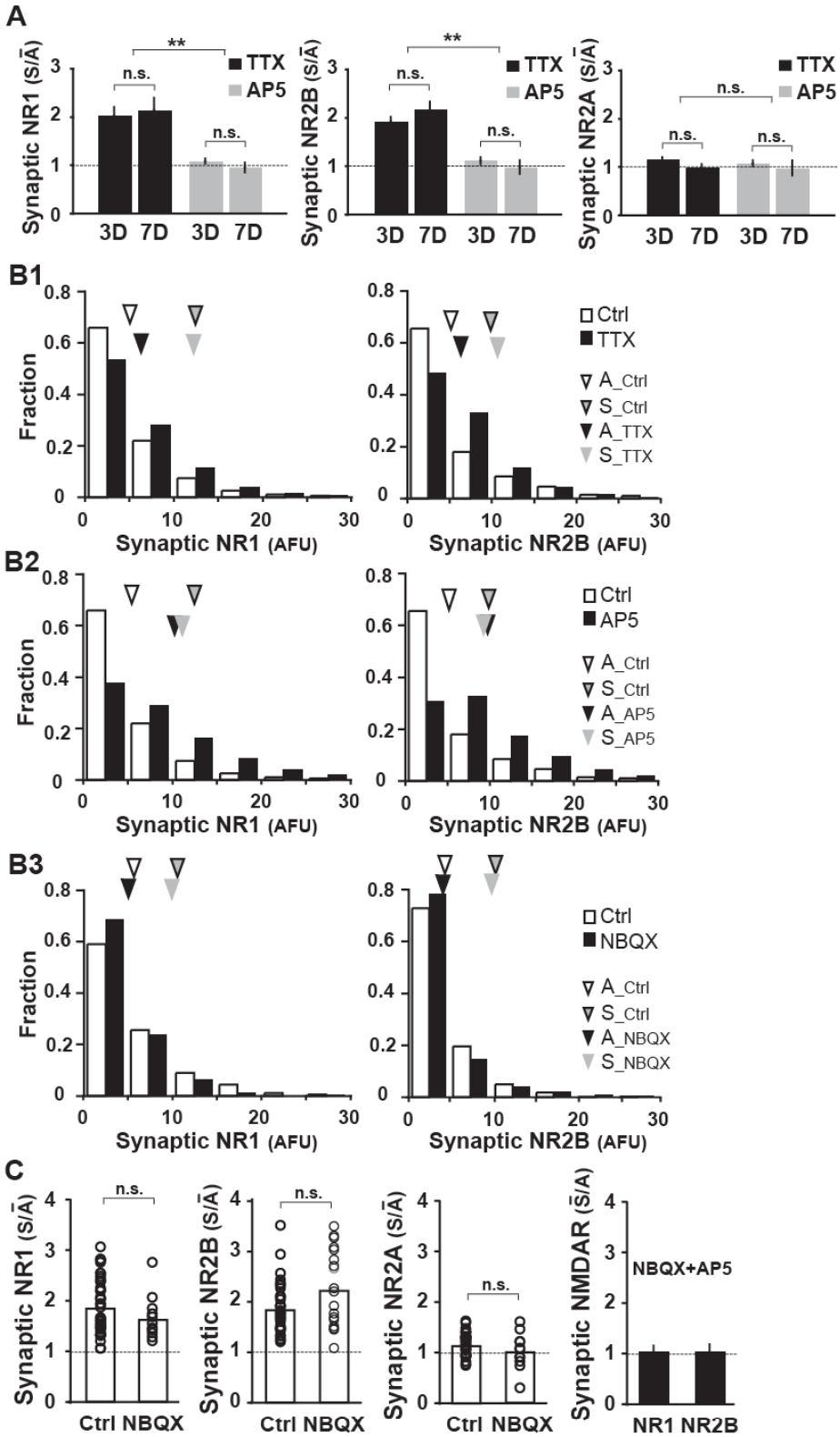

(A) Ongoing spontaneous release and NMDAR activation mediates the synapse-specific suppression of NR1/NR2B at active synapses**.** Prolonged blockade of action potentials (TTX) or NMDARs (AP5) was begun either at the point of TeNT infection (7D blockade) or 4 days after TeNT infection (3D blockade). Neurons were fixed and stained 7 days after TeNT infection. Under both paradigms, NR1 accumulated at silenced synapses in the presence of TTX, but failed to accumulate in the presence of AP5. **p < 0.01; n.s., not significant. Like NR1, NR2B accumulated at silenced synapses in the presence of TTX but failed to accumulate in the presence of AP5 under both 7 day blockade (7D) and 3 day blockade (3D) paradigms. **p < 0.01; n.s., not significant. NR2A shows no differential accumulation at silenced synapses under 7 day (7D) or 3 day (3D) blockade with TTX or AP5. n.s., not significant.

(B) Relative differences in the activation of NMDARs by synaptic release drive selective changes in NMDAR composition. Histograms show the integrated intensity of NR1 (left) and NR2B (right) at active (A) and silenced (S) synapses after chronic treatment with TTX (B1), D-AP5 (B2), or NBQX (B3). (B1) TTX treatment causes a small global increase in NR1 and NR2B content but preserves the differential accumulation of NR1/NR2B at silenced synapses. (B2) Chronic AP5 causes a global increase in NMDAR content that erases the differential accumulation of NR1/NR2B at silenced synapses. (B3) NBQX has little effect on global NMDAR content and does not affect the selective accumulation of NR1/NR2B at silenced synapses. Arrowheads indicate means. AFU, arbitrary fluorescence units.

(C) AMPAR blockade does not affect NMDAR accumulation at silenced synapses. Similar to control conditions (Ctrl), silenced synapses accumulate NR1 and NR2B but not NR2A in the presence of the AMPAR antagonist NBQX (10 μM, 7 days). $S/\overline{A}$: $NR1_{NBQX}$, 2.1 ± 0.5, n = 13 neurons; $NR2B_{NBQX}$, 2.4 ± 0.2, n = 21; $NR2A_{NBQX}$, 1.0 ± 0.1,

n = 11. n.s., not significant. Similar to AP5 alone (Figure 3), simultaneous blockade of AMPARs (NBQX) and NMDARs (AP5) equalizes synaptic NR1 and NR2B content between active and silenced synapses. $S/\overline{A}$: $NR1_{NBQX+AP5}$, 1.1 ± 0.1, n = 11 neurons; $NR2B_{NBQX+AP5}$, 1.0 ± 0.2, n = 8.

Figure S4, related to Figure 6.

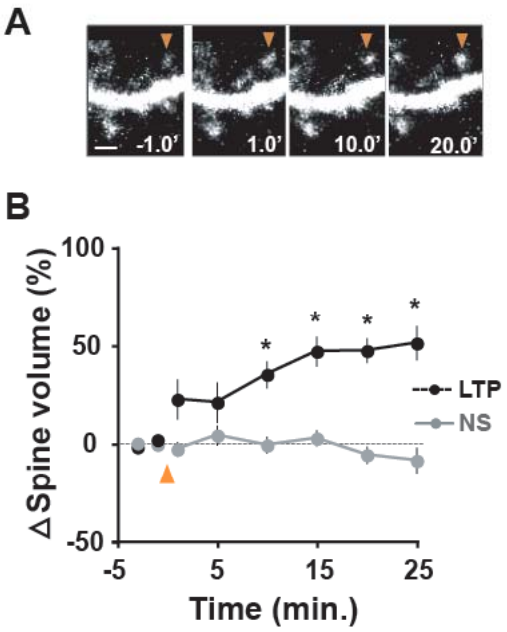

(A) LTP induction by two-photon glutamate uncaging triggers sustained spine growth at single synapses. Shown are images of spines on a stretch of hippocampal neuron dendrite. Spine enlargement occurs at the stimulated spine (orange arrowheads), but not at non-stimulated neighboring spines. Scale bar, 1 μm.

(B) Quantitative analyses of spine volume changes over time following LTP induction. Spine enlargement persists for at least 25 min (153 ± 9% at 25 min post LTP induction, n = 8). Stimulated spines (LTP, black); NS, non-stimulated neighboring spine; *$p < 0.05$. Orange arrowhead indicates time of repeated glutamate uncaging to induce LTP.

SUPPLEMENTAL EXPERIMENTAL PROCEDURES

Neuron Culture, Viral Transduction, and Transfection

Hippocampal neuron cultures were prepared from E18 rat embryos and maintained for 19-22 days *in vitro* (DIV) as described (Ehlers et al., 2007). Hippocampal neurons were infected with lentivirus expressing SphGFP-IRES-TeNT on DIV11-12. At DIV17-19, one week after infection, neurons were transfected with pCMV5-mCherry using Lipofectamine 2000 (Invitrogen) for two days to allow visualization of postsynaptic neurons. Immunostaining and electrophysiological recordings were performed at DIV19-21. Global activity manipulations were begun with drug addition (in mM: 0.002 TTX, 0.05 AP5) either at the point of TeNT infection (7 days blockade) or 4 days after TeNT infection (3 days blockade). Since these two conditions produced no significant difference in synaptic NMDAR accumulation, pooled data were represented in Figure 3. NMDAR accumulation segregated between 7 days and 3 days blockade are shown in Figure S5. For NBQX (0.02 mM) and NBQX/AP5, drugs were applied for 7 days. Unless otherwise mentioned, the same concentration of TTX (0.002 mM) and AP5 (0.05 mM) was applied either chronically or acutely throughout the experiments.

FM Dye Loading Assays

FM dye loading was performed on hippocampal neurons expressing synaptophysin-EGFP (SphGFP) or SphGFP-IRES-TeNT to assay synaptic release in a bouton-by-bouton manner. Two different protocols were applied to monitor either evoked or spontaneous release at individual boutons. For evoked release, high potassium solution (50 mM KCl with 0.01 mM FM 4-64) was applied for 60 sec to allow for depolarization-evoked synaptic release and uptake of FM 4-64. Spontaneous release was assayed by FM 4-64 uptake after 15 min of loading under conditions that permitted spontaneous release but prevented action potentials (0.002 mM TTX, 0 Ca^{2+}, 0.01 mM FM 4-64). Following FM loading, cells were washed extensively before imaging.

Immunocytochemistry and Antibodies

Hippocampal cultures were fixed with 4% paraformaldehyde/4% sucrose. To label the total pool of receptors, fixed cells were permeabilized with -20°C methanol and 0.1% Triton X-100 in PBS prior to primary antibody incubation. Fixed and permeabilized

neurons were blocked with 5% BSA/10% goat-serum for 8 hrs at 4°C, and then incubated with mouse anti-NR1 (Affinity BioReagents), rabbit anti-NR2A (Millipore), or mouse anti-NR2B (BD Bioscience) for 8 hrs at 4°C. To selectively label surface NMDARs, fixed cells were fixed and blocked without permeabilization. After blocking, fixed cells were incubated with rabbit anti-NR2A (44-58) or rabbit anti-NR2B (46-60) (gifts from F. Anne Stephenson, University of London, London, UK) for 30 min at room temperature. After incubating with primary antibodies, cells were washed with PBS and then incubated with Alexa 647-conjugated secondary antibodies (Molecular Probes) for 1 hr at room temperature. Cells were then washed with PBS and mounted onto glass slides with 5-10 μl of mounting solution (Electron Microscopy Science) for imaging.

Image Analysis and Quantification

To measure the synaptic content of NR1, NR2A and NR2B, circular regions with a diameter of 0.7 μm were selected based on the center of individual spine heads. For each neuron analyzed, regions were first chosen blindly through all spines and then classified into SphGFP-positive and SphGFP-negative groups, corresponding to silenced synapses (S) and active synapses (A), respectively. Regions were then transferred to the corresponding NMDAR channel and the integrated fluorescence intensity of NMDAR subunit antibody labeling measured at individual spines. Background intensity was measured from 25-30 random background regions and subtracted from measured values of integrated intensity. Synaptic content measured from silenced synapses was normalized to the mean synaptic content at active synapses ($S/\overline{A}$, 200~500 active synapses per neuron) on the same neuron. The $S/\overline{A}$ value thus describes how molecular content at a silenced synapse differs from the average content at active synapses on the same cell. The mean $S/\overline{A}$ was also calculated for individual neurons for each NMDAR subunit. The spatial range of NMDAR accumulation at or near individual silenced synapses was determined by measuring the normalized NR1 or NR2B content at synapses along a 30 μm long stretch of dendrite centered by a silenced synapses. The time course of NMDAR accumulation or loss was determined by measuring NR1 and NR2B synaptic content following AP5 washout. Postsynaptic neurons contacted by active and TeNT-silenced boutons were first kept in medium containing TTX (0.002 mM) plus AP5 (0.02 mM) for 3 days to normalize synaptic NMDAR content and then switched to TTX only for 6, 12, or 24 hours prior to fixation and immunostaining for NR1 and NR2B. Unless

otherwise stated, error bars represent the standard error of the mean and statistical comparisons were Student's t tests.

RNA Interference

Expression of two NR2B shRNA sequences (#1: 5′CCCGGATGAGTCCTCCATGTTCTT CAAGAGAGAACATGGAGGACTCATCCTTTTTGGAAAC3' (Kim et al., 2005); #2: 5'CCG GGCTATGGCATTGCTATCCAAACTCGAGTTTGGATAGCAATGCCATAGCTTTT TG3' (Open Biosystems, #RMM3981-98062524)) and a scrambled shRNA control were cloned into lentiviral expression systems. For effective knockdown of NR2B expression, 3-5 days of expression was allowed in both 293T cells and hippocampal neurons. In 293T cells, expression of NR2A and NR2B was performed by transfection of pRK5-NR2A or pRK5-NR2B, respectively.

uEPSC Recordings, Calcium Imaging, and Plasticity Induction

Two-photon glutamate uncaging and uEPSC recordings. Voltage clamp whole-cell recordings from hippocampal neurons were performed with pipettes (4-6 MΩ) containing Cs-based internal solution (in mM): 135 $CsMeSO_3$, 10 HEPES, 10 Na-phosphocreatine, 4 $MgCl_2$, 4 Na_2-ATP, 0.4 Na-GTP, 3 ascorbate. Recordings were obtained using a multiclamp 700B amplifier and filtered at 2 kHz. Local uncaging stimulation was delivered on the tip of spine heads (~0.5 μm from the center of the spine head in the direction away from the dendritic shaft) and uEPSCs were recorded from the soma. uEPSCs were recorded at -70 mV ($uEPSC_{-70mV}$) to measure the contribution of AMPARs and at +40 mV ($uEPSC_{+40mV}$) to measure mixed AMPAR- and NMDAR-mediated synaptic currents. NMDAR-uEPSCs were extracted from $uEPSC_{+40mV}$ by measuring $uEPSC_{+40mV}$ amplitude 45 ms after the $uEPSCs_{-70mV}$ peak. In each experiment, pairs of two nearby spines of similar volume, one silenced and the other active, were chosen for uEPSC recordings. To estimate the fraction of NR2B-containing receptors at individual synapses, uEPSC recordings were performed following application of the NR2B selective antagonist ifenprodil (3 μM, Tocris) or Ro25-6891 (1 μM, Tocris).

Two-photon glutamate uncaging and Ca^{2+} imaging. Ca^{2+} imaging was performed as described previously (Harvey and Svoboda, 2007; Lee et al., 2009; Yasuda et al., 2004) on pairs of nearby spines (one silenced and one neighboring active synapse). Whole-cell patch clamp recordings from hippocampal neurons were obtained using electrodes containing Ca^{2+}-sensitive dye (500 μM Fluo-4FF) and Ca^{2+}-insensitive dye (300 μM Alexa-594) in Cs^{+} internal solution. Images were acquired every 16 ms in frame-scan mode. The uncaging-evoked Ca^{2+} transients were measured as the change in green fluorescence (ΔG) divided by red fluorescence (R), normalized to $(G/R)_{MAX}$ measured in 10 mM Ca^{2+} ($[\Delta G/R] / [G/R]_{MAX} * K_{D,Fluo\text{-}4FF}$)(Yasuda et al., 2004). Thapsigargin (1 μM) and ryanodine (20 μM) were included in the internal solution to block Ca^{2+} release from intracellular stores (Harvey and Svoboda, 2007). In control experiments, Ca^{2+} transients were measured in the presence of ifenprodil (3 μM) or D-AP5 (50 μM).

Potentiation of AMPAR-uEPSCs. To probe LTP threshold, one target spine (active or silenced) was subjected to plasticity induction protocols and compared to a non-stimulated neighboring spine (NS). AMPAR-uEPSCs were measured before and after LTP-inducing or subthreshold stimuli in 5 min intervals. The LTP-inducing protocol consisted of postsynaptic depolarization to 0 mV paired with 30 uncaging pulses of 4 ms duration at 0.5 Hz (Harvey and Svoboda, 2007). The subthreshold protocol consisted of postsynaptic depolarization to 0 mV paired with 20 uncaging pulses of 1 ms duration at 0.5 Hz. Only cells stably held for at least 20 min after stimulation were included in the analysis.

Spine enlargement. Pairs of spines (A+NS or S+NS) were chosen and subject to glutamate uncaging stimulation for plasticity induction. The spine volume indicated by mCherry fluorescence intensity was measured before and after uncaging stimuli. For these experiments, 0 Mg^{2+} was used to prevent NMDAR block. For each experiment, image z stacks were acquired before and after plasticity induction every 5 min for 30 min. Spine volumes were measured as the integrated mCherry fluorescence after background subtraction. The LTP-inducing protocol consisted of 30 uncaging pulses of 4 ms duration at 0.5 Hz (Harvey and Svoboda, 2007). The subthreshold protocols consisted of 20 uncaging pulses of 1 ms duration at 0.5 Hz. Changes in spine volume upon uncaging stimulation were described by the fractional change in mCherry fluorescence intensity

given by $(F-F_0)/F_0$ where F is the measured intensity at any given time t and F_0 is the measured intensity at time zero.

SUPPLEMENTAL REFERENCES

Ehlers, M.D., Heine, M., Groc, L., Lee, M.C., and Choquet, D. (2007). Diffusional trapping of GluR1 AMPA receptors by input-specific synaptic activity. Neuron *54*, 447-460.

Harvey, C.D., and Svoboda, K. (2007). Locally dynamic synaptic learning rules in pyramidal neuron dendrites. Nature *450*, 1195-1200.

Kim, M.J., Dunah, A.W., Wang, Y.T., and Sheng, M. (2005). Differential roles of NR2A-and NR2B-containing NMDA receptors in Ras-ERK signaling and AMPA receptor trafficking. Neuron *46*, 745-760.

Lee, S.J., Escobedo-Lozoya, Y., Szatmari, E.M., and Yasuda, R. (2009). Activation of CaMKII in single dendritic spines during long-term potentiation. Nature *458*, 299-304.

Yasuda, R., Nimchinsky, E.A., Scheuss, V., Pologruto, T.A., Oertner, T.G., Sabatini, B.L., and Svoboda, K. (2004). Imaging calcium concentration dynamics in small neuronal compartments. Sci STKE *2004*, pl5.